[CANCER RESEARCH 64, 5712–5719, August 15, 2004]

Pathophysiological Effects of Vascular Endothelial Growth Factor Receptor-2-Blocking Antibody plus Fractionated Radiotherapy on Murine Mammary Tumors

Bruce M. Fenton, Scott F. Paoni, and Ivan Ding

Department of Radiation Oncology, University of Rochester Medical Center, Rochester, New York

ABSTRACT

Although clinical trials of antiangiogenic strategies have been disappointing when administered as single agents, such approaches can play an important role in cancer treatment when combined with conventional therapies. Previous studies have shown that DC101, an antiangiogenic monoclonal antibody against vascular endothelial growth factor receptor-2, can produce significant growth inhibition in spontaneous and transplanted tumors but can also induce substantial hypoxia. Because DC101 appears to potentiate radiotherapy in some tumors, the present studies were undertaken to characterize pathophysiological changes following combined therapy and to determine whether radioresponse is enhanced despite the induction of hypoxia. MCa-4 and MCa-35 mammary carcinomas were treated with: (*a*) DC101; (*b*) 5 × 6 Gy radiation fractions; or (*c*) the combination. Image analysis of frozen tumor sections was used to quantitate: (*a*) hypoxia; (*b*) spacing of total and perfused blood vessels; and (*c*) endothelial and tumor cell apoptosis. For MCa-4, combination treatment schedules produced significant and prolonged delays in tumor growth, whereas single-modality treatments had minor effects. For MCa-35, radiation or the combination led to equivalent growth inhibition. In all tumors, hypoxia increased markedly after either radiation or DC101 alone. Although combination therapy produced no immediate pathophysiological changes, hypoxia ultimately increased after cessation of therapy. Preferential increases in endothelial apoptosis following combination treatment suggest that in addition to blocking tumor angiogenesis, DC101 enhances radiotherapy by specifically sensitizing endothelial cells, leading to degeneration of newly formed blood vessels.

INTRODUCTION

Combinations of conventional treatments such as radiotherapy or chemotherapy with antiangiogenic therapy have been suggested as promising alternatives to single-agent therapy, with the goal of specifically targeting both tumor cell and vascular compartments (1–6). In preclinical models, such combinations have shown greater than additive effects due to apparent mutual potentiation of these approaches. A promising hypothesis is that these synergistic effects could arise through inhibition of the stimulatory effects of radiation on angiogenesis, which would then restrain tumor regrowth after irradiation (7).

Radiation research has traditionally concentrated primarily on the tumor cell compartment, with much less attention paid to either the effects of radiotherapy on the endothelial cell compartment or, more recently, the pathophysiological mechanisms leading to synergistic combinations of antiangiogenic agents and radiotherapy. The effects of radiotherapy on tumor vascular growth are complex because they depend on a competing balance between angiogenic and antiangiogenic factors. *In vitro* studies have shown that radiotherapy can act as both angiogenic promoter and potent antiangiogenic agent. Radiotherapy can inhibit endothelial cell survival, proliferation, tube formation and invasion (3, 8) and directly induce endothelial apoptosis (9, 10). Although tumor growth is initially inhibited, angiogenic growth factors are at the same time up-regulated, leading to a secondary burst in angiogenesis and tumor cell proliferation. Radiotherapy can specifically up-regulate vascular endothelial growth factor (VEGF) receptor-2 in endothelial cells (3) and VEGF in tumor cells (3, 11), thereby inducing endothelial proliferation, migration, and tube formation (12). VEGF is also a known survival factor for endothelial cells, induces antiapoptotic pathways, promotes tumor regrowth, and serves as a radioprotector (3).

Tumor oxygenation can increase or decrease following single-dose radiation (13–15), and fractionated radiotherapy can induce similar changes, depending on the extent to which tumor reoxygenation occurs (16, 17). If tumors do not reoxygenate but instead become more hypoxic during therapy, both VEGF (18, 19) and VEGF receptor (20) levels will be further up-regulated, shifting the tumor toward a more angiogenic phenotype that may be counterproductive to treatment success. Thus, tumor cells can protect their associated vasculature from radiation damage, both directly and indirectly. This protective role can possibly be countered by co-administration of angiogenesis inhibitors, but the question then arises as to whether the antiangiogenic treatments themselves will compromise conventional therapy through reductions in oxygen delivery and decreased tumor radiosensitivity.

Previous results have been inconclusive. SU6668, an inhibitor of the VEGF, platelet-derived growth factor, and fibroblast growth factor receptors, causes tumor blood flow to first decrease then increase to higher than control levels at 24 h posttherapy (21). One interpretation of these data is that the reduction in tumor perfusion caused by SU6668 results in hypoxic stress, thereby leading to later induction of VEGF transcription. VEGF is also known to induce nitric oxide production, thus leading to increases in vascular permeability and vasodilation, which may explain why blood perfusion was transiently elevated. Surprisingly, although blood flow subsequently decreased to 75% of control, concomitant radiotherapy was still potentiated by SU6668.

It has been hypothesized that antiangiogenic agents may serve to normalize the ineffective tumor vasculature, thereby improving delivery of oxygen and drugs (22). However, various reports have shown increases (23, 24), decreases (4, 25, 26), or no effect at all (5) on tumor oxygenation and blood flow following such strategies. Our previous work has shown that DC101, an antibody against VEGF receptor-2, can produce significant growth inhibition in both spontaneous and transplanted murine mammary tumors (27). Perfused vascular counts were reduced, however, ultimately leading to tumor hypoxia, necrosis, and apoptosis. Because DC101 has also been reported to potentiate radiotherapy in other preclinical models (5, 25), the present studies were undertaken to characterize the microregional, pathophysiological consequences of such combined therapy. A key question was whether radioresponse would be enhanced despite the observed increase in tumor hypoxia following DC101 alone.

Received 2/9/04; revised 6/8/04; accepted 6/16/04.

Grant support: NIH Grant CA52586.

The costs of publication of this article were defrayed in part by the payment of page charges. This article must therefore be hereby marked *advertisement* in accordance with 18 U.S.C. Section 1734 solely to indicate this fact.

Requests for reprints: Bruce M. Fenton, Box 704, University of Rochester Medical Center, Rochester, NY 14642. E-mail: bruce.fenton@rochester.edu.

MATERIALS AND METHODS

Tumor Models

Tumor cells from MCa-4 or MCa-35 murine mammary carcinomas (obtained from Dr. Luka Milas, MD Anderson Cancer Center) were inoculated into the hind legs of 6–8-week-old female C3H/HeJ mice. The MCa-4 is a poorly vascularized, hypoxic, well-differentiated tumor, whereas the MCa-35 is well vascularized, more evenly oxygenated, poorly-differentiated, and more metastatic (27, 28). Tumor volumes were estimated by the formula: volume $= \pi d^3/6$, where d is the diameter of the leg plus tumor, as measured using calipers. Tumor volumes were corrected by subtracting the volume of the nontumor leg. Guidelines for the humane treatment of animals were followed as approved by the University Committee on Animal Resources.

$DiOC_7$ Perfusion Marker and EF5 Hypoxic Marker

To visualize blood vessels open to flow, $DiOC_7$, an intravascular stain that preferentially stains cells immediately adjacent to the vessels, was injected i.v. 1 min before freezing (29). Localized areas of tumor hypoxia were assessed in 9.0-μm frozen tumor sections by immunohistochemical identification of sites of 2-nitroimidazole metabolism (30). A pentafluorinated derivative of etanidazole (EF5) was injected i.v. (0.2 ml of 10 mM EF5) 1 h before tumor freezing (31). Regions of high EF5 metabolism were visualized using a Cy3 fluorochrome (Amersham Biosciences) conjugated to the ELK3-51 antibody, which is extremely specific for the EF5 adducts that form when the drug is incorporated by hypoxic cells (32). Both the EF5 (made by the National Cancer Institute) and the ELK3-51 were obtained from the University of Pennsylvania Imaging Service Center.

DC101 Administration

Anti-VEGF receptor-2 [DC101; kindly supplied by ImClone Systems (New York, NY)] was given i.p. every 3 days at 45 mg/kg, beginning at 4 days postimplantation (early initiation, tumor volume ~190 mm^3 for MCa-4; ~75 mm^3 for MCa-35; and ~100 mm^3 for the extended treatment MCa-4) or 7 days postimplantation (late initiation, tumor volume ~ 380 mm^3). An equal volume of saline was administered to control mice.

Fractionated Irradiation

Irradiations were performed on nonanesthetized mice using a ^{137}Cs source operating at 3.0 Gy/min. Mice were confined to a plastic jig with tumor-bearing legs extended through an opening in the side, allowing tumors to be locally irradiated. Total doses of either 30 or 60 Gy were administered in 5 or 10 daily fractions of 6 Gy (omitting weekends).

Immunohistochemistry and Image Acquisition

Tumor sections were imaged using a ×10 objective, digitized (QImaging Retiga 1300C peltier-cooled, 12-bit digital camera), background-corrected, and image-analyzed using Image Pro software (Media Cybernetics, Silver Spring, MD; Ref. 30). Color image montages from 16 adjacent microscope fields (encompassing a total area of 21.6 mm^2) were automatically acquired and digitally combined under four different staining conditions. First, images of the $DiOC_7$ were obtained immediately after the sections were sliced on the cryostat. After staining, the same section was returned to identical stage coordinates, and images of EF5/Cy3 and either anti-CD31 (in MCa-4 tumors) or panendothelial cell antigen (in MCa-35) were acquired (PharMingen).

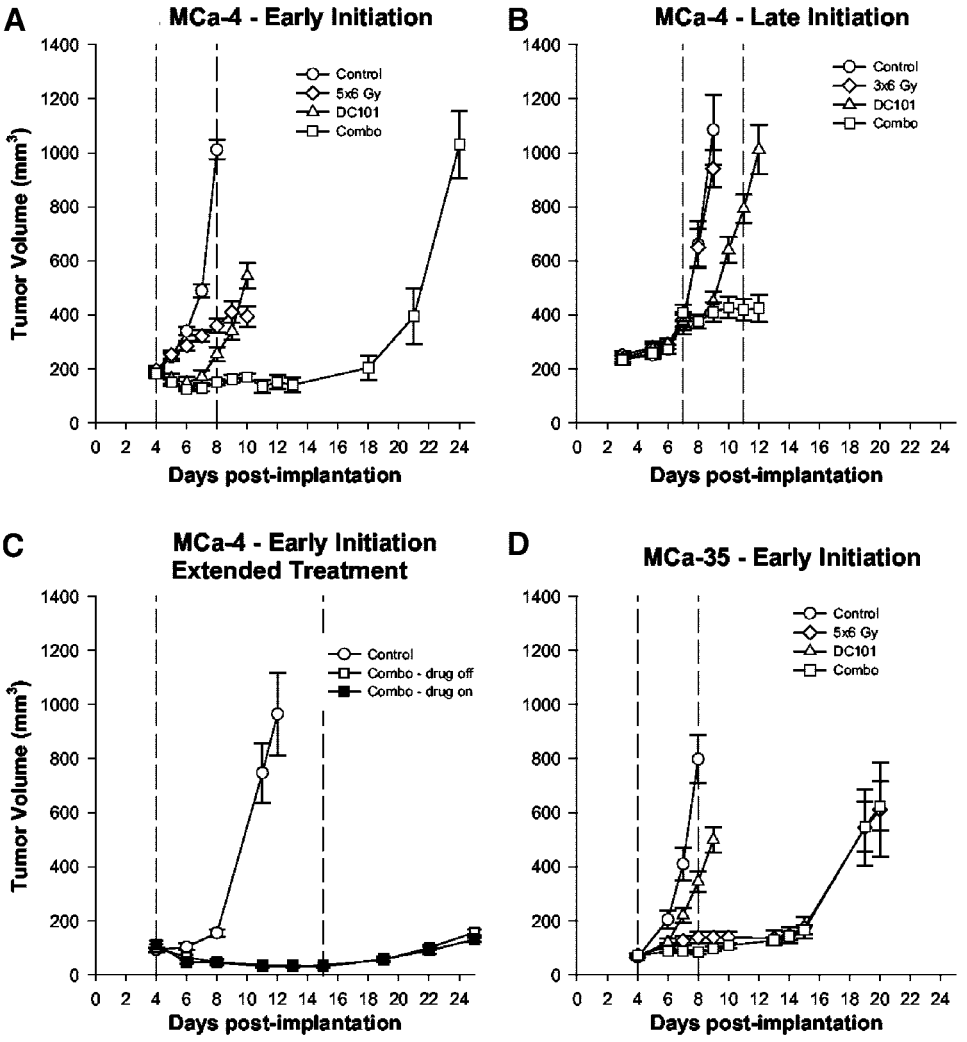

Fig. 1. Effect of single and combined treatments on tumor growth inhibition (mean ± SE; 10 tumors/group). ○, controls; ◇, radiotherapy alone; △, DC101 alone; □, *combo*, radiotherapy and DC101; and *vertical dashed lines*, treatment beginning and end times. *A*, MCa-4 tumors, early initiation treatment (begun at volumes ~190 mm^3). *B*, MCa-4 tumors, late initiation treatment (begun at volumes ~380 mm^3); note that radiotherapy was terminated after only three fractions in this case due to the rapid tumor growth. *C*, MCa-4 tumors, early initiation extended treatment (begun at volumes ~100 mm^3 and continued for 2 weeks); □, tumors in which treatment was terminated after 2 weeks. *D*, MCa-35 tumors, early initiation treatment (begun at volumes ~75 mm^3).

Finally, sections were stained and imaged for H&E. In separate frozen sections, CD31 endothelial staining was followed by apoptosis staining using a FITC terminal deoxynucleotidyltransferase-mediated nick end labeling assay (Promega), and images were acquired at ×20.

Image Analysis

Zonal Hypoxia Analysis. To quantitate microregional hypoxia as a function of distance from perfused blood vessels, zonal analysis methods were used as described in detail previously (33). In brief, $DiOC_7$ (3) images were color segmented to identify perfused blood vessels, and a "distance filter" was applied, which replaces the intensity of each pixel with an intensity proportional to the distance of that pixel from the nearest perfused vessel. This distance-filtered image was successively thresholded and binarized to select regions of the image within specific zones around perfused vessels. Finally, these binary masks were multiplied by the corresponding EF5/Cy3 images to determine the mean EF5/Cy3 intensities within each zone.

Vascular Spacing, Apoptosis, and Necrosis. As described previously (27), tumor blood vessel spacing was determined using a combination of image segmentation and distance map filtering to obtain a spatial sampling of the distance map intensities, which are directly proportional to the distribution of distances to the nearest vessel. Tumor blood vessel spacing is reflective of the median distance over which oxygen and nutrients must diffuse to reach all cells of the tumor. Colocalized images of CD31 staining and apoptosis were obtained by dilating the CD31 masks by 2 μm and using a logical "AND" image arithmetic operation with the apoptosis mask to select and count either perivascular or tumor cell apoptotic events. Regions of gross necrosis were visually selected on the H&E images and outlined with the Image Pro multiple area of interest tool for determination of percent area.

Statistical Analysis

Tumor means were compared using the Student's *t* test or the Mann-Whitney Rank Sum test and were considered significant for $P \leq 0.05$. Slopes and intercepts of the zonal analyses were compared using multiple linear regressions on log transformed EF5 intensities.

RESULTS

Tumor Growth Inhibition. Fig. 1 presents tumor growth curves for all experiments. Because tumor pathophysiology can vary as a function of tumor volume, growth curves were not necessarily followed to completion; instead tumors were frozen to obtain comparable tumor volumes among treatments and controls. For early initiation MCa-4 treatments, control tumors were frozen at either small (400 ± 20 mm^3) or large (1050 ± 40 mm^3) tumor volumes, and combination-treated tumors were frozen at 210 ± 20 mm^3 and 1130 ± 100 mm^3 (Fig. 1*A*). All treatments resulted in inhibition of tumor growth but with distinct differences. For radiotherapy, tumor growth was repressed to some extent, but volumes progressively increased during treatment. For DC101, tumor progression was delayed for 3 days after the first dose, but showed little or no response

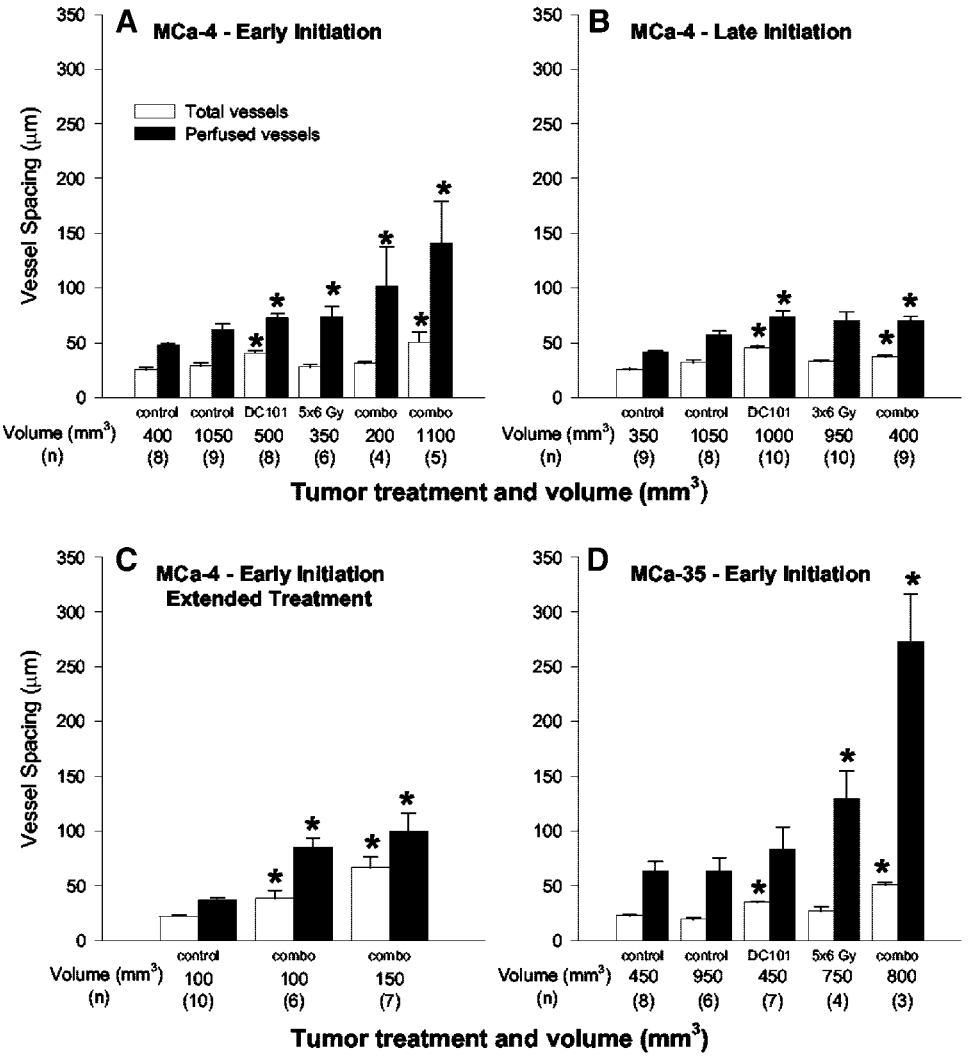

Fig. 2. Effect of treatment on total and perfused blood vessel spacing (mean ± SE). Tumor volumes and numbers of tumors in each group are indicated below the appropriate columns. *, statistically significant differences in relation to volume-matched controls ($P \leq 0.05$). *A*, early initiation MCa-4 tumors; all treatment groups were frozen at day 2 posttherapy, except the 1100 mm^3 combination tumors, which were allowed to grow for 16 days posttherapy. *B*, late initiation MCa-4 tumors. DC101 and combination (*combo*) tumors were frozen 1 d posttherapy, radiotherapy tumors were frozen after three fractions. *C*, combination tumors were frozen at day 7 or 10 posttherapy. *D*, DC101 tumors were frozen 1 d posttherapy; combination and radiotherapy tumors were frozen at day 12 posttherapy.

to the second dose at day 7. Finally, the combination treatment totally suppressed tumor growth, continuing for up to 10 days posttherapy.

For late initiation MCa-4 treatments (Fig. 1*B*), fractionated radiotherapy alone had no significant effect and was discontinued following only three fractions, due to the large tumor volumes. DC101 delayed tumor progression for only 1 day. Again, the combination almost totally suppressed tumor growth until tumor freezing. To gauge the pathophysiological effects of extended therapy, combination therapy was also administered for 2 weeks to a third set of MCa-4 tumors (Fig. 1*C*), and again, combination treated tumors demonstrated essentially no growth. This group was further subdivided into a "drug off" group that received DC101 only during the fractionated radiotherapy and a "drug on" group that received DC101 for 10 more days following radiotherapy. Both regimens produced significant growth inhibition with no significant differences between the two.

Fig. 1*D* summarizes results for the early initiation MCa-35 tumors. Although growth rates were similar between MCa-35 and MCa-4 controls, response to DC101 was less pronounced in the MCa-35, despite the smaller initial tumor volumes. Responses to radiotherapy and the combination were similar, and both markedly suppressed tumor growth for up to 7 days posttherapy.

Total and Perfused Vessel Spacing. Total and perfused vessel spacings are summarized in Fig. 2. For early initiation MCa-4 tumors (Fig. 2*A*), controls were frozen at small and large volumes (400 and 1050 mm^3), and treated tumors were frozen at 2 days following monotherapies and at both 2 and 16 days following the combination. Compared with volume-matched controls, total vessel spacing was significantly increased only for DC101 tumors and the recovered combination group (1100 mm^3), whereas perfused vessel spacing was significantly increased after all treatments. For late initiation MCa-4 (Fig. 2*B*), DC101 and the combination significantly increased both total and perfused vessel spacing at 1 d posttherapy, but at a significantly reduced level compared with early initiation ($P = 0.04$). In line with its minimal effects on tumor growth rate, radiotherapy had no significant effects on total or perfused vessel spacing. Following extended combination therapy (Fig. 2*C*), both total and perfused spacing were significantly increased at 7 days posttherapy with no increase in tumor volume, indicating a reduction in both total and perfused vessel densities. By 10 days posttherapy, volumes were only slightly larger, and total vessel spacing was even further increased.

In MCa-35 tumors (Fig. 2*D*), DC101 had no effect on perfused vessel spacing, but significantly increased total vessel spacing ($P < 0.001$). Perfused spacing was significantly higher for both radiotherapy tumors ($P = 0.04$) and the combination ($P < 0.001$), however, by the time tumors resumed growth at day 20 posttherapy. Although perfused spacing in the combination MCa-35 tumors was much higher than in MCa-4, the somewhat later time point for the MCa-35 may have allowed these tumors to outgrow their vasculature to a somewhat greater extent.

Overall Hypoxia. Although either DC101 or radiotherapy significantly increased overall hypoxia in early initiation MCa-4 tumors, surprisingly, the combination had no initial effect (see 200 mm^3

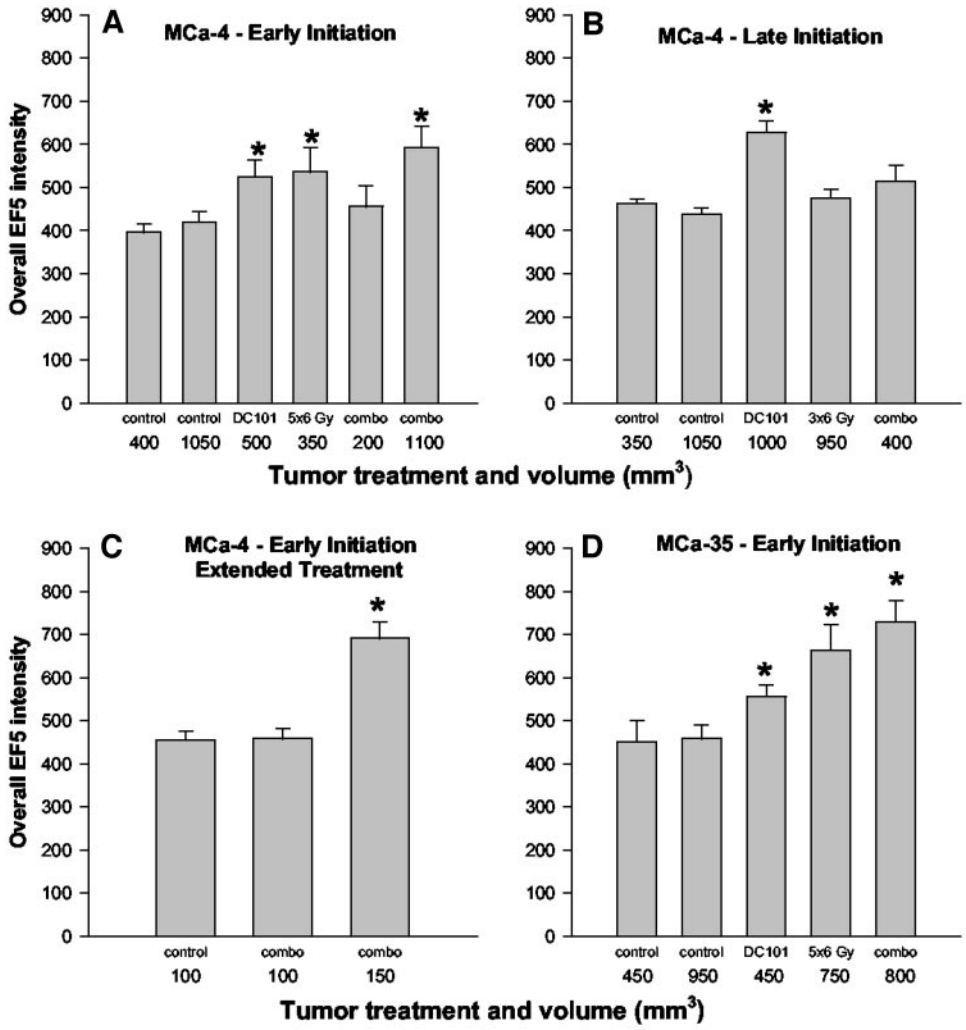

Fig. 3. Effect of treatment on overall changes in hypoxia (mean EF5/Cy3 intensity). *A–D* correspond to the same treatment classes of Fig. 2; ∗, statistically significant differences in relation to volume-matched controls. Tumor numbers are as shown in Fig. 2; *combo*, radiotherapy and DC101.

combination tumors in Fig. 3*A*). By 16 days posttherapy, however, when volumes were 1100 mm^3, the combination tumors had become significantly more hypoxic. For late initiation MCa-4 tumors (Fig. 3*B*), frozen 1 day posttherapy, only DC101 significantly increased hypoxia, but no late time point was available for the combination-treated tumors. The lack of response in the late initiation radiotherapy tumors, which was also evident in the tumor growth and vessel spacing results, may relate to the fact that these tumors were likely more hypoxic to begin with than the early initiation, and therefore also more radioresistant. For the extended treatment tumors (Fig. 3*C*), overall hypoxia was unchanged at 7 days postcombination treatment but significantly increased when tumor growth resumed 3 days later ($P < 0.001$). For the MCa-35 tumors (Fig. 3*D*), hypoxia increased significantly following either radiotherapy or the combination, and tumors were frozen when tumor growth resumed at day 20 post-therapy.

Zonal Analysis of Hypoxia. To visualize spatial heterogeneities in hypoxia, Fig. 4 presents EF5/Cy3 intensities as a function of distance from the nearest blood vessel, each point corresponding to the median intensity within a specific 20-μm-wide zone. Because EF5/Cy3 intensities averaged over the first 20-μm zone are closely related to intravascular oxygen levels, hypoxia changes at these perivascular distances are reflective of alterations in oxygen delivery capacity or functionality. Thus, flatter slopes correspond to a relatively uniform distribution of oxygen, whereas steeper slopes reflect increasing oxygen diffusional limitations. Both large and small control tumors exhibited fairly flat slopes in all plots (Fig. 4, *A–D*), indicating a relatively homogeneous distribution of oxygen. Small volume controls were not substantially different from large volume, suggesting that in these cases, tumor cells have not as yet outgrown their oxygen supply. For the early initiation MCa-4 tumors (Fig. 4*A*), DC101 produced a significant increase in perivascular EF5 intensities ($P = 0.007$). In contrast, perivascular hypoxia in combination-treated tumors varied from roughly equivalent to controls at 2 days posttreatment to significantly more hypoxic 2 weeks later, indicating a decrease in vascular functionality with recovery from treatment. Comparing slopes, an even more striking decrease in the ability of the blood vessels to adequately supply the tumor with oxygen is apparent following either DC101 or radiotherapy alone (Fig. 4*A*). Instead of the relatively homogeneous distribution of hypoxia seen with control tumors, both monotherapies produced a substantial increase in hypoxia with increasing distance from the vessels. The curves for combination tumors, however, are quite similar to controls immediately following treatment, but markedly steeper 2 weeks later. For late initiation MCa-4 (Fig. 4*B*), only DC101 produced significant increases in both perivascular hypoxia and slope. Following extended treatment (Fig. 4*C*), curves were unchanged at 7 days posttherapy (Fig. 4*C*, *sml combo*), but substantially higher 3 days later (Fig. 4*C*, *med combo*), indicating a rapid decrease in vascular function.

For early initiation MCa-35 (Fig. 4*D*), DC101 curves remained fairly flat, but were shifted to slightly more hypoxic levels. For these tumors, radiotherapy and the combination were each so effective that almost 3 weeks were required before the tumors progressed to the minimal size

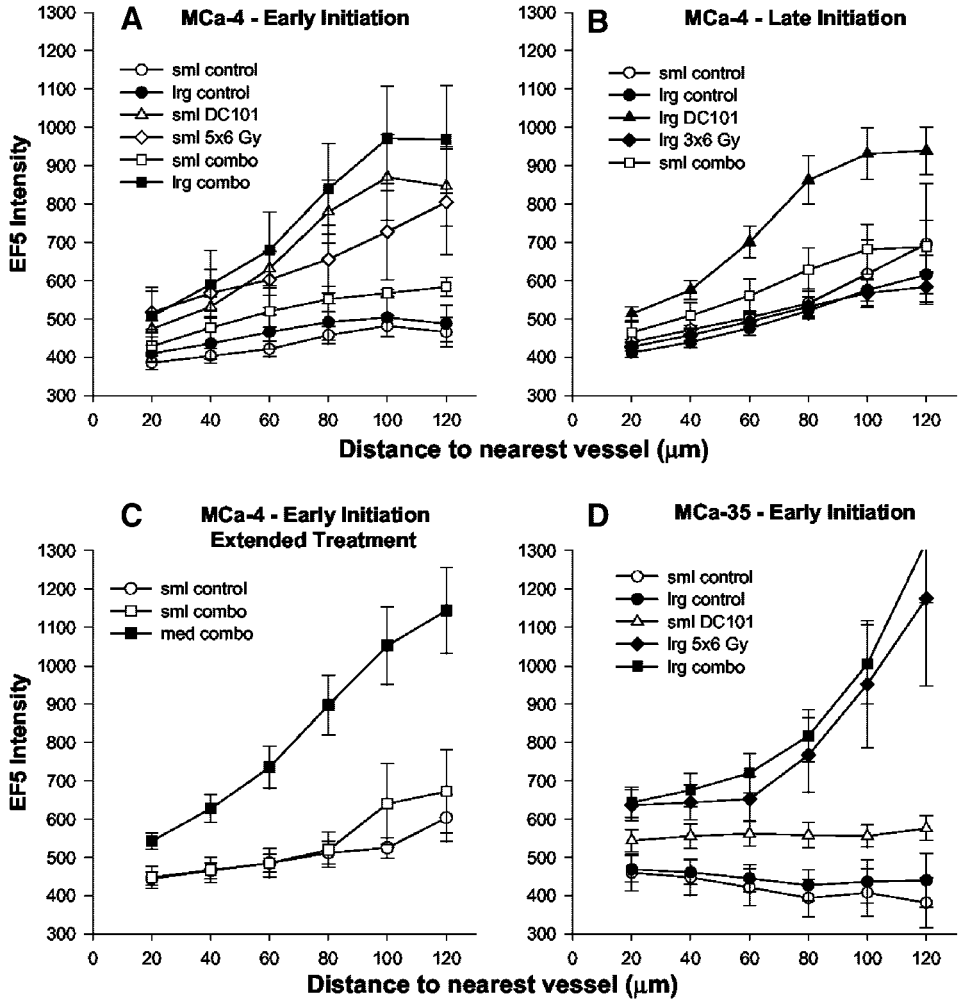

Fig. 4. Changes in tumor hypoxia as a function of distance from nearest total blood vessel. In all panels, smaller tumors (*sml;* ~350 mm^3) are denoted by *open symbols*, whereas larger tumors (*lrg;* ~850 mm^3) are denoted by *filled symbols; circles* are controls, *diamonds* are radiotherapy alone, *triangles* are DC101 alone, and *squares* are the combination. *A–D* correspond to the same treatments, tumor volumes, and numbers of tumors as shown in Fig. 2.

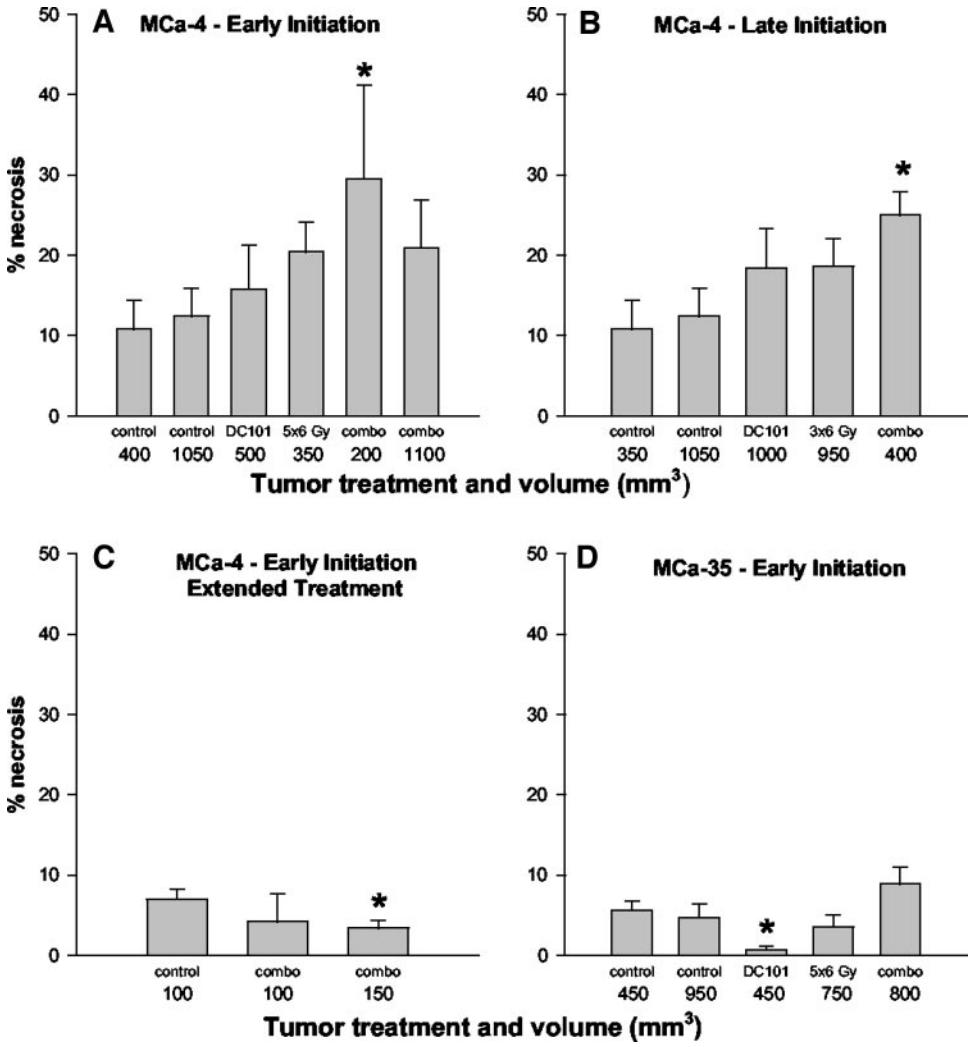

Fig. 5. Percentage overall necrosis. *A–D* correspond to the same treatment classes and tumor numbers of Fig. 2; ∗, statistically significant differences in relation to volume-matched controls; *combo*, radiotherapy and DC101.

needed for analysis. By that time, perivascular hypoxia was significantly increased, and slopes were markedly steeper for both regimens.

Percentage Necrosis. Fig. 5 demonstrates that hypoxia does not necessarily associate with increased necrosis. Although the early combination-treated MCa-4 tumors were significantly more necrotic ($P = 0.05$, Fig. 5*A*), neither DC101 nor radiotherapy alone had any substantial effect. In late initiation MCa-4 (Fig. 5*B*), combination treatment again resulted in significantly higher necrosis, even at fairly small volumes ($P = 0.008$). Following extended combination treatment, minimal necrosis was observed (Fig. 5*C*). Although percentage necrosis was fairly similar between MCa-4 and MCa-35 controls, response to combination treatment was minimal in the case of the MCa-35 (Fig. 5*D*).

Tumor and Endothelial Cell Apoptosis. Fig. 6 illustrates changes in the numbers of apoptotic tumor and endothelial cells for the early initiation MCa-4 tumors. All treatments significantly increased the numbers of apoptotic tumor cells, but the combination produced the most substantial rise. For endothelial cells, in contrast, only the combination produced a significant increase, suggesting a sensitization of the endothelial cells with this combined regimen.

DISCUSSION

Numerous investigators have shown synergistic effects when combining radiation with antiangiogenic agents, although results regarding the optimal timing of treatment have been inconclusive. Initial reports demonstrated improved radiocurability in combination with TNP-470, but only if the drug was administered at the end of fractionated radiotherapy (34). Later studies showed that treatment with an antibody to VEGF before single-dose irradiation resulted in a greater than additive effect (11). *In vitro* studies demonstrated that endothelial cell killing by radiation was potentiated by anti-VEGF but that tumor cell radioresponse was unaffected, suggesting that blood vessels may be the primary target. More recent studies have reported somewhat conflicting results. Concurrent administration of angiostatin and radiotherapy was most beneficial (1), but SU5416 or SU6668 improved treatment equally whether administered before or after radiotherapy (35) or fractionated radiation (6), suggesting that increased tumor oxygenation was probably not the primary factor in improving radioresponse.

In neuroblastoma xenografts, treatment with either DC101 or 6 Gy radiation led to increased tumor hypoxia, as determined polarographically (25). Following combination treatment, hypoxia was slightly reduced, but tumors were still significantly more hypoxic than controls. Similarly, combinations of fractionated radiotherapy with either SU11248 or SU5416 served to decrease tumor blood flow (6, 36), and maintenance of SU11248 following combination therapy produced a clear improvement in tumor control. This contrasts with current results, in which no additional enhancement was found when tumors

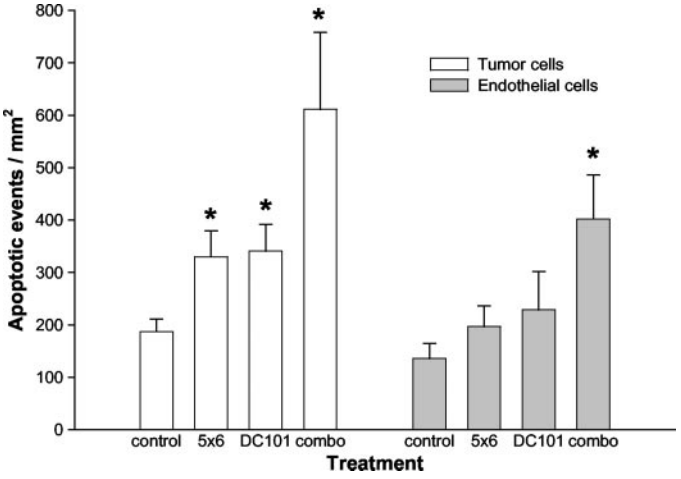

Fig. 6. Changes in the numbers of apoptotic tumor (□) and endothelial (▨) cells for the early initiation MCa-4 tumors. All tumor volumes ranged from 300–400 mm^3, and treated tumors were frozen at 2 days posttherapy. *, statistically significant differences in relation to volume-matched controls; *5×6*, 5 × 6 Gy radiation fractions; *combo*, radiotherapy and DC101.

were maintained on DC101 following the combination, although SU11248 inhibits both VEGF receptor-2 and platelet-derived growth factor receptor, and maintenance therapy was somewhat shorter in the current study.

Combination therapy is clearly much more effective than either radiotherapy or DC101 in suppressing growth in MCa-4 tumors. For late initiation tumors, radiotherapy had almost no effect, whereas DC101 slightly slowed tumor growth. In marked contrast, the combination totally blocked tumor progression for weeks beyond completion of 1- or 2-week therapies. In MCa-35 tumors, tumors were much more sensitive to radiotherapy alone, and it was impossible to gauge whether DC101 provided additional benefit. The lack of a synergistic effect in these tumors could be related to: (*a*) alterations in the balance of angiogenic and antiangiogenic cytokines; (*b*) the increased radiosensitivity of the MCa-35; or (*c*) the fact that treatment was initiated at somewhat smaller tumor volumes than for the MCa-4.

Although early or late initiation monotherapy with either DC101 or radiotherapy increased both perfused vessel spacing and overall hypoxia, changes following combined therapies were somewhat more complex. Perfused vessel spacing increased, but in the absence of a corresponding increase in hypoxia. Bruns *et al.* (4) reported a somewhat similar phenomena, whereby hypoxia increased significantly following DC101 alone, but decreased when combined with gemcitabine. They hypothesized that the development of new blood vessels was not yet required in their smaller combination-treated tumors, because tumor cells were still within the oxygen diffusion distance of preexisting host vessels. Although overall hypoxia was unchanged in MCa-4 tumors following the combination, necrosis was significantly higher, suggesting that: (*a*) the ability of the vessels to supply oxygen is clearly compromised; and (*b*) the tumor cells become progressively more necrotic following extended hypoxia. Given the fact that growth of the combination-treated tumors was constrained to quite small tumor volumes for either early initiation, late initiation, or extended treatment regimens, the most likely reason that hypoxia does not initially increase in these tumors is that they have not as yet had a chance to outgrow their DC101-compromised vasculature, due to the additional tumor antiproliferative effects of the radiotherapy. Even at these relatively small tumor volumes, regions of hypoxia were almost exclusively limited to areas immediately adjacent to necrosis, which were also furthest from the surrounding host vasculature.

A likely mechanism for the effectiveness of the combination treatment is that DC101 serves to inhibit the ability of VEGF to act as a survival factor for endothelial cells (37), thus sensitizing the vessels to radiation damage (6). Although tumor cell apoptosis in MCa-4 tumors was increased by each treatment, the combination produced the most striking effects and was the only regimen that significantly increased endothelial cell apoptosis. Because perfused vessel spacing increased following the combination, with no change in tumor volume, perfused vessels were clearly eliminated during therapy. Two weeks postcombination therapy, when the tumors had substantially increased in volume, total and perfused vessel spacing as well as overall hypoxia were markedly increased. Because total and perfused perivascular hypoxia also increased, blood flow was most likely compromised in these remaining vessels. At this time, however, it cannot be conclusively stated whether: (*a*) total or functional vessels are destroyed by the treatment; (*b*) vessel growth was simply delayed allowing the tumor to outgrow the functional vasculature; or (*c*) some combination of the two occurred. In any case, the net result was an increase in localized islands of tumor hypoxia with accompanying necrosis following treatment recovery.

Previous work has shown increases in both tumor cell and endothelial apoptosis following DC101 alone, although following substantially longer treatment times (38). Immature, non-pericyte-coated vessels have also been shown to be more susceptible to damage by antiangiogenic agents (39), although it is as yet uncertain whether the same holds true following radiotherapy. Because these neovessels are probably not yet as effective in delivering blood flow and oxygen, specifically targeting them could lead to a decrease in perfused vessel density without markedly influencing functional vessel density. Furthermore, damaged immature vessels may be unable to progress to a more functional phenotype, and adjacent tumor cells would gradually outgrow their nutrient supply, ultimately leading to the observed increase in necrosis. Although oxygenation in these expanding necrotic regions would clearly be reduced, overall measurements of tumor hypoxia using EF5 binding are constrained to viable regions of the tumor, which are more relevant to radioresponse. Because overall hypoxia remained relatively constant following combination treatment, radiosensitivity would not be expected to be compromised. Recent work somewhat contradicts this mechanism as the sole determinant, however, because response to the combination of fractionated radiotherapy plus VEGF receptor-2 inhibition was most effective when delivered postirradiation (40). Given that concomitant administration resulted in no improvement, endothelial cell radiosensitization may be a less important component of response in some tumors, although vessels damaged by irradiation could also remain sensitive to later VEGF receptor-2 inhibition (40).

The present results also highlight the importance of tumor implantation site in evaluating tumor pathophysiological response. Compared with mammary fat-pad implantations (27), tumor growth rates in the leg implants were 2–3-fold higher in both control and DC101-treated tumors. In the leg tumors, angiogenic vessels can presumably sprout from abundant, preexisting, host vessels that supply the leg muscle, leading to well-vascularized, oxygenated tumors. In the fat-pad, however, the host tissue is less vascularized, and the tumor is more dependent on neovessel development to supply its metabolic needs. Accordingly, MCa-4 vessel counts were much higher in the leg-implanted tumors than in the fat-pad, leading to a more uniform distribution of oxygen. In the MCa-35, in contrast, vessel counts were comparatively lower in the leg implants. In this environment, localized levels of angiogenic growth factors may be more important in promoting sufficient expansion of the tumor vasculature. Interestingly, although DC101 produced similar tumor growth inhibition at both sites, significantly more hypoxia was induced in leg implants in each tumor model. Although combination therapy had no immediate

detrimental effects on tumor oxygenation, tumor necrosis was significantly increased, and tumors became substantially more hypoxic following cessation of treatment. It remains to be seen whether tumors will remain well oxygenated throughout an even more extended 6–8-week course of fractionated radiotherapy or eventually become hypoxic and whether radiotherapy fraction sizes can be further reduced in combination with DC101 while maintaining similar growth delays. Furthermore, more detailed studies are clearly warranted to address these questions as well as to optimize scheduling with anti-angiogenic strategies.

REFERENCES

1. Gorski DH, Mauceri HJ, Salloum RM, et al. Potentiation of the antitumor effect of ionizing radiation by brief concomitant, exposures to angiostatin. Cancer Res 1998; 58:5686–9.
2. Mauceri HJ, Hanna NN, Beckett MA, et al. Combined effects of angiostatin and ionizing radiation in antitumour therapy. Nature 1998;394:287–91.
3. Abdollahi A, Lipson KE, Han X, et al. SU5416 and SU6668 attenuate the angiogenic effects of radiation-induced tumor cell growth factor production and amplify the direct anti-endothelial action of radiation in vitro. Cancer Res 2003;63:3755–63.
4. Bruns CJ, Shrader M, Harbison MT, et al. Effect of the vascular endothelial growth factor receptor-2 antibody DC101 plus gemcitabine on growth, metastasis and angiogenesis of human pancreatic cancer growing orthotopically in nude mice. Int J Cancer 2002;102:101–8.
5. Kozin SV, Boucher Y, Hicklin DJ, Bohlen P, Jain RK, Suit HD. Vascular endothelial growth factor receptor-2-blocking antibody potentiates radiation-induced long-term control of human tumor xenografts. Cancer Res 2001;61:39–44.
6. Geng L, Donnelly E, McMahon G, et al. Inhibition of vascular endothelial growth factor receptor signaling leads to reversal of tumor resistance to radiotherapy. Cancer Res 2001;61:2413–9.
7. Sonveaux P, Brouet A, Havaux X, et al. Irradiation-induced angiogenesis through the up-regulation of the nitric oxide pathway: implications for tumor radiotherapy. Cancer Res 2003;63:1012–9.
8. Trinh T, Abdollahi A, Krempien R, Hlatky L, Lipson KE, Huber PE. SU5416 and SU6668 decrease angiogenic effects of radiation-induced factor productions by tumor cells and amplify the direct anti-endothelial action of radiation in vitro. Int J Radiat Oncol Biol Phys 2003;57:S319.
9. Paris F, Fuks Z, Kang A, et al. Endothelial apoptosis as the primary lesion initiating intestinal radiation damage in mice. Science 2001;293:293–7.
10. Garcia-Barros M, Paris F, Cordon-Cardo C, et al. Tumor response to radiotherapy regulated by endothelial cell apoptosis. Science 2003;300:1155–9.
11. Gorski DH, Beckett MA, Jaskowiak NT, et al. Blockade of vascular endothelial growth factor stress response increases the antitumor effects of ionizing radiation. Cancer Res 1999;59:3374–8.
12. Neufeld G, Cohen T, Gengrinovitch S, Poltorak Z. Vascular endothelial growth factor (VEGF) and its receptors. FASEB J 1999;13:9–22.
13. Sonveaux P, Dessy C, Brouet A, et al. Modulation of the tumor vasculature functionality by ionizing radiation accounts for tumor radiosensitization and promotes gene delivery. FASEB J 2002;16:1979–81.
14. Fenton BM. Effects of carbogen plus fractionated irradiation on KHT tumor oxygenation. Radiother Oncol 1997;44:183–90.
15. Fenton BM, Paoni SF, Koch CJ, Lord EM. Effect of local irradiation on tumor oxygenation, perfused vessel density, and development of hypoxia. Adv Exp Med Biol 1998;454:619–28.
16. Petersen C, Eichler W, Frommel A, et al. Proliferation and micromilieu during fractionated irradiation of human FaDu squamous cell carcinoma in nude mice. Int J Radiat Biol 2003;79:469–77.
17. Lyng H, Tanum G, Evensen JF, Rofstad EK. Changes in oxygen tension during radiotherapy of head and neck tumours. Acta Oncol 1999;38:1037–42.
18. Allalunis-Turner MJ, Franko AJ, Parliament MB. Modulation of oxygen consumption rate and vascular endothelial growth factor mRNA expression in human malignant glioma cells by hypoxia. Br J Cancer 1999;80:104–9.
19. Laderoute KR, Alarcon RM, Brody MD, et al. Opposing effects of hypoxia on expression of the angiogenic inhibitor thrombospondin 1 and the angiogenic inducer vascular endothelial growth factor. Clin Cancer Res 2000;6:2941–50.
20. Veikkola T, Karkkainen M, Claesson-Welsh L, Alitalo K. Regulation of angiogenesis via vascular endothelial growth factor receptors. Cancer Res 2000;60:203–12.
21. Griffin RJ, Williams BW, Wild R, Cherrington JM, Park H, Song CW. Simultaneous inhibition of the receptor kinase activity of vascular endothelial, fibroblast, and platelet-derived growth factors suppresses tumor growth and enhances tumor radiation response. Cancer Res 2002;62:1702–6.
22. Jain RK. Normalizing tumor vasculature with anti-angiogenic therapy: a new paradigm for combination therapy. Nat Med 2001;7:987–9.
23. Fenton BM, Paoni SF, Grimwood BG, Ding I. Disparate effects of endostatin on tumor vascular perfusion and hypoxia in two murine mammary carcinomas. Int J Radiat Oncol Biol Phys 2003;57:1038–46.
24. Hansen-Algenstaedt N, Stoll BR, Padera TP, et al. Tumor oxygenation in hormone-dependent tumors during vascular endothelial growth factor receptor-2 blockade, hormone ablation, and chemotherapy. Cancer Res 2000;60:4556–60.
25. Gong H, Pottgen C, Stuben G, Havers W, Stuschke M, Schweigerer L. Arginine deiminase and other antiangiogenic agents inhibit unfavorable neuroblastoma growth: potentiation by irradiation. Int J Cancer 2003;106:723–8.
26. Denis F, Colas S, Chami L, et al. Changes in tumor vascularization after irradiation, anthracyclin, or antiangiogenic treatment in nitrosomethyl ureas-induced rat mammary tumors. Clin Cancer Res 2003;9:4546–52.
27. Fenton BM, Paoni SF, Ding I. Effect of VEGF receptor-2 antibody on vascular function and oxygenation in spontaneous and transplanted tumors. Radiother Oncol 2004;72:221–30.
28. Milas L, Wike J, Hunter N, Volpe J, Basic I. Macrophage content of murine sarcomas and carcinomas: associations with tumor growth parameters and tumor radiocurability. Cancer Res 1987;47:1069–75.
29. Trotter MJ, Chaplin DJ, Olive PL. Use of a carbocyanine dye as a marker of functional vasculature in murine tumours. Br J Cancer 1989;59:706–9.
30. Fenton BM, Paoni SF, Lee J, Koch CJ, Lord EM. Quantification of tumor vascular development and hypoxia by immunohistochemical staining and HbO_2 saturation measurements. Br J Cancer 1999;79:464–71.
31. Fenton BM, Lord EM, Paoni SF. Effects of radiation on tumor intravascular oxygenation, vascular configuration, hypoxic development, and survival. Radiat Res 2001; 155:360–8.
32. Lord EM, Harwell L, Koch CJ. Detection of hypoxic cells by monoclonal antibody recognizing 2-nitroimidazole adducts. Cancer Res 1993;53:5721–6.
33. Fenton BM, Paoni SF, Beauchamp BK, Ding I. Zonal image analysis of tumour vascular perfusion, hypoxia, and necrosis. Br J Cancer 2002;86:1831–6.
34. Murata R, Nishimura Y, Hiraoka M. An antiangiogenic agent (TNP-470) inhibited reoxygenation during fractionated radiotherapy of murine mammary carcinoma. Int J Radiat Oncol Biol Phys 1997;37:1107–13.
35. Ning S, Laird D, Cherrington JM, Knox SJ. The antiangiogenic agents SU5416 and SU6668 increase the antitumor effects of fractionated irradiation. Radiat Res 2002; 157:45–51.
36. Schueneman AJ, Himmelfarb E, Geng L, et al. SU11248 maintenance therapy prevents tumor regrowth after fractionated irradiation of murine tumor models. Cancer Res 2003;63:4009–16.
37. Gupta VK, Jaskowiak NT, Beckett MA, et al. Vascular endothelial growth factor enhances endothelial cell survival and tumor radioresistance. Cancer J 2002;8:47–54.
38. Sweeney P, Karashima T, Kim SJ, et al. Anti-vascular endothelial growth factor receptor 2 antibody reduces tumorigenicity and metastasis in orthotopic prostate cancer xenografts via induction of endothelial cell apoptosis and reduction of endothelial cell matrix metalloproteinase type 9 production. Clin Cancer Res 2002;8: 2714–24.
39. Gee MS, Procopio WN, Makonnen S, Feldman MD, Yeilding NM, Lee WM. Tumor vessel development and maturation impose limits on the effectiveness of anti-vascular therapy. Am J Pathol 2003;162:183–93.
40. Zips D, Krause M, Hessel F, et al. Experimental study on different combination schedules of VEGF-receptor inhibitor PTK787/ZK222584 and fractionated irradiation. Anticancer Res 2003;23:3869–76.